

Bounding the plastic strength of polycrystalline solids by linear-comparison homogenization methods

BY MARTÍN I. IDIART^{1,2,*}

¹*Departamento de Aeronáutica, Facultad de Ingeniería, Universidad Nacional de La Plata, Avda. 1 esq. 47, La Plata B1900TAG, Argentina*

²*Consejo Nacional de Investigaciones Científicas y Técnicas (CONICET), CCT La Plata, Calle 8 N° 1467, La Plata B1904CMC, Argentina*

The elastoplastic response of polycrystalline metals and minerals above their brittle–ductile transition temperature is idealized here as rigid–perfectly plastic. Bounds on the overall plastic strength of polycrystalline solids with prescribed microstructural statistics and single-crystal plastic strength are computed by means of a linear-comparison homogenization method recently developed by Idiart & Ponte Castañeda (Idiart & Ponte Castañeda 2007 *Proc. R. Soc. A* **463**, 907–924 (doi:10.1098/rspa.2006.1797)). Hashin–Shtrikman and self-consistent results are reported for cubic and hexagonal polycrystals with varying degrees of crystal anisotropy. Improvements over earlier linear-comparison bounds are found to be modest for high-symmetry materials but become appreciable for low-symmetry materials. The largest improvement is observed in self-consistent results for low-symmetry hexagonal polycrystals, exceeding 15 per cent in some cases. In addition to providing the sharpest bounds available to date, these results serve to evaluate the performance of the aforementioned linear-comparison method in the context of realistic material systems.

Keywords: polycrystals; plasticity; homogenization

1. Motivation

The elastoplastic response of polycrystalline metals and minerals above their brittle–ductile transition temperature is to a great extent dictated by the morphology, lattice orientation and elastoplastic response of each individual single-crystal grain composing the aggregate. Relating the macroscopic response with the microscopic properties is necessary to estimate the deformation-induced plastic anisotropy that develops in these materials when subjected to large deformations, a problem relevant to various engineering applications such as metal-forming processes—see the monograph by Kocks *et al.* (1998). Very often the response of these materials is idealized as elastically rigid and plastically

*martin.idiart@ing.unlp.edu.ar

non-hardening. Within this the so-called rigid–perfectly plastic model, the above problem reduces to finding the macroscopic yield surface of the polycrystal given the yield surface at the single-crystal level and the statistics of the morphology and orientation distributions of the grains. Owing to their inherent microstructural randomness, cognate polycrystalline solids do not exhibit a single response but a—hopefully narrow—range of responses. Therefore, one can either develop estimates that yield a single representative response or derive bounds for the entire range of possible responses. This work is concerned with bounds. Bounds are also useful for two additional reasons: they provide benchmarks to test estimates and they can be used as estimates themselves.

The simplest bounds for the yield surface of polycrystalline solids are the outer bound of Taylor (1938) and the inner bound of Reuss (1929). Their extremal character was proved by Bishop & Hill (1951). These elementary bounds are obtained by assuming uniform strain-rate and uniform stress fields in the classical minimum energy principles, and make use of one-point microstructural statistics only. They have proved useful in the context of high-symmetry polycrystalline solids—like face-centred cubic solids—where the heterogeneity contrast is low, but as crystal anisotropy increases their predictions diverge and become highly inaccurate. This fact has motivated the development of refined bounds that can incorporate higher order microstructural statistics. Most of those bounds have been derived in the context of nonlinear viscoplasticity, which includes rigid-perfect plasticity as a limiting case. The first bounds for polycrystalline solids that account for two-point statistics were derived by Dendievel *et al.* (1991) via the nonlinear Hashin–Shtrikman procedure initially proposed by Willis (1983) and developed further by Talbot & Willis (1985). A more general method inspired by the linear-comparison procedure of Ponte Castañeda (1991) was later proposed by deBotton & Ponte Castañeda (1995) and developed further by Ponte Castañeda & Suquet (1998). This linear-comparison method allows the use of any available bound for linearly elastic polycrystals to produce bounds for nonlinear viscoplastic polycrystals, thus having the potential of incorporating higher order statistics. The optimal linearization is obtained via suitably designed variational principles. This linear-comparison method was applied to cubic and hexagonal polycrystals by Nebozhyn *et al.* (2000, 2001) and Liu & Ponte Castañeda (2004), who showed that the linear-comparison predictions for rigid–perfectly plastic polycrystals improve significantly over the elementary predictions of Taylor and Reuss, especially when crystal anisotropy is large. In addition, their results served to demonstrate the inconsistency of an ‘incremental’ theory of polycrystalline plasticity proposed by Hill (1965) and Hutchinson (1976), which was found to violate the bounds. More recently, Lebensohn *et al.* (2011) have reported linear-comparison bounds for (two-phase) voided polycrystals and have shown that ‘tangent’ theories of polycrystalline plasticity such as those proposed by Molinari *et al.* (1987), Lebensohn & Tomé (1993) and Bornert *et al.* (2001) can also violate bounds.

Idiart & Ponte Castañeda (2007*a*) have recently shown that the linear-comparison methods of deBotton & Ponte Castañeda (1995) and Ponte Castañeda & Suquet (1998) make implicit use of a relaxation in their linearization scheme which weakens the resulting bounds. Eliminating this relaxation leads to sharper bounds but increases the computational complexity. Idiart & Ponte Castañeda (2007*a,b*) derived non-relaxed linear-comparison bounds and applied

them to a model material consisting of a porous single crystal with cylindrical symmetry under anti-plane loading. They found that the improvement over the relaxed bounds increased with increasing number of crystal slip systems, being as much as 10 per cent in some extreme cases. Motivated by these developments, the method of Idiart & Ponte Castañeda (2007a) is used in this work to bound the plastic strength of a fairly general class of polycrystalline solids made of cubic and hexagonal single crystals with varying degrees of plastic anisotropy. In addition to providing the sharpest bounds available to date for polycrystalline plastic solids, these results are used to evaluate the performance of the non-relaxed linear-comparison method in the context of realistic material systems.

2. The polycrystalline solid model

Polycrystals are idealized here as random aggregates of perfectly bonded single crystals (i.e. grains). Individual grains are assumed to be of a similar size, much smaller than the specimen size and the scale of variation of the applied loads. Furthermore, the aggregates are assumed to have statistically uniform and ergodic microstructures. Attention is restricted here to monolithic polycrystals, even though the methodologies considered in the next section can handle multi-phase systems equally well.

Plasticity is most conveniently studied by adopting an Eulerian description of motion; the ensuing analysis thus refers to the *current* configuration of the aggregate at a generic stage of deformation. Let the grain orientations take on a set of N discrete values, characterized by rotation tensors $\mathbf{Q}^{(r)}$ ($r = 1, \dots, N$). All grains with a given orientation $\mathbf{Q}^{(r)}$ occupy a disconnected domain $\mathcal{Q}^{(r)}$ and are collectively referred to as ‘phase’ r . The domain occupied by the polycrystal is then $\mathcal{Q} = \cup_{r=1}^N \mathcal{Q}^{(r)}$. Volume averages over the aggregate \mathcal{Q} and over each phase $\mathcal{Q}^{(r)}$ will be denoted by $\langle \cdot \rangle$ and $\langle \cdot \rangle^{(r)}$, respectively. The domains $\mathcal{Q}^{(r)}$ can be described by a set of characteristic functions $\chi^{(r)}(\mathbf{x})$, which take the value 1 if the position vector \mathbf{x} is in $\mathcal{Q}^{(r)}$ and 0 otherwise. In view of the microstructural randomness, the functions $\chi^{(r)}$ are random variables that must be characterized in terms of ensemble averages (Willis 1977). The ensemble average of $\chi^{(r)}(\mathbf{x})$ represents the one-point probability $p^{(r)}(\mathbf{x})$ of finding phase r at \mathbf{x} ; the ensemble average of the product $\chi^{(r)}(\mathbf{x})\chi^{(s)}(\mathbf{x}')$ represents the two-point probabilities $p^{(rs)}(\mathbf{x}, \mathbf{x}')$ of finding simultaneously phase r at \mathbf{x} and phase s at \mathbf{x}' . Higher order probabilities are defined similarly. Owing to the assumed statistical uniformity and ergodicity, the one-point probability $p^{(r)}(\mathbf{x})$ can be identified with the volume fractions—or concentrations— $c^{(r)} = \langle \chi^{(r)}(\mathbf{x}) \rangle$ of each phase r , the two-point probability $p^{(rs)}(\mathbf{x}, \mathbf{x}')$ can be identified with the volume average $\langle \chi^{(r)}(\mathbf{x})\chi^{(s)}(\mathbf{x}') \rangle$, and so on. Note that $\sum_{r=1}^N c^{(r)} = 1$.

Grains are assumed to individually deform by multi-glide along K slip systems following a rigid–perfectly plastic response. In accordance with standard crystal plasticity theory, their *strength domains* are given by the convex sets

$$P^{(r)} = \{ \boldsymbol{\sigma} : |\boldsymbol{\sigma} \cdot \boldsymbol{\mu}_{(k)}^{(r)}| \leq \tau_0^{(k)}, k = 1, \dots, K \}, \quad (2.1)$$

where $\tau_0^{(k)} > 0$ is the yield strength of the k th slip system in a ‘reference’ crystal and

$$\boldsymbol{\mu}_{(k)}^{(r)} = \frac{1}{2}(\mathbf{n}_{(k)}^{(r)} \otimes \mathbf{m}_{(k)}^{(r)} + \mathbf{m}_{(k)}^{(r)} \otimes \mathbf{n}_{(k)}^{(r)}) \tag{2.2}$$

are second-order Schmid tensors with $\mathbf{n}_{(k)}^{(r)}$ and $\mathbf{m}_{(k)}^{(r)}$ denoting the unit vectors normal to the slip plane and along the slip direction of the k th system, respectively, for a crystal with orientation $\mathbf{Q}^{(r)}$. The Schmid tensors of a given phase r are related to corresponding tensors $\boldsymbol{\mu}_{(k)}$ for the ‘reference’ crystal via $\boldsymbol{\mu}_{(k)}^{(r)} = \mathbf{Q}^{(r)\top} \boldsymbol{\mu}_{(k)} \mathbf{Q}^{(r)}$. Note that the Schmid tensors are traceless and therefore the strength domains (2.1) are insensitive to hydrostatic stresses. The boundary $\partial P^{(r)}$ of the set $P^{(r)}$ represents the *yield surface* of phase r . Plastic flow of the grains is governed by the so-called normality rule.

The macroscopic plastic strength of the polycrystalline aggregate corresponds to the set of stress states that can produce macroscopic plastic flow. Homogenizing the relevant field equations, Suquet (1983) and Bouchitté & Suquet (1991) showed that the macroscopic plastic strength can be characterized by an *effective strength domain* defined as

$$\tilde{P} = \{\bar{\boldsymbol{\sigma}} : \exists \boldsymbol{\sigma}(\mathbf{x}) \in \mathcal{S}(\bar{\boldsymbol{\sigma}}) \text{ and } \boldsymbol{\sigma}(\mathbf{x}) \in P^{(r)} \text{ in } \Omega^{(r)}, r = 1, \dots, N\}, \tag{2.3}$$

where $\bar{\boldsymbol{\sigma}}$ denote the macroscopic stress states that produce macroscopic plastic flow, $\boldsymbol{\sigma}(\mathbf{x})$ are the underlying microscopic stress fields, and

$$\mathcal{S}(\bar{\boldsymbol{\sigma}}) = \{\boldsymbol{\sigma}(\mathbf{x}) : \text{div } \boldsymbol{\sigma}(\mathbf{x}) = \mathbf{0} \text{ in } \Omega, \langle \boldsymbol{\sigma}(\mathbf{x}) \rangle = \bar{\boldsymbol{\sigma}}\} \tag{2.4}$$

is the set of statically admissible stress fields with volume average $\bar{\boldsymbol{\sigma}}$. The effective strength domain depends on the *crystallographic* texture of the polycrystal through the set of orientations $\mathbf{Q}^{(r)}$ and concentrations $c^{(r)}$, and on the *morphological* texture through the ensemble averages of the characteristic functions $\chi^{(r)}(\mathbf{x})$ of the domains $\Omega^{(r)}$. Note that convexity of the sets $P^{(r)}$ implies convexity of \tilde{P} . The boundary $\partial \tilde{P}$ of the set \tilde{P} represents the *effective yield surface* of the polycrystalline solid, surface that we seek to bound.

3. Linear-comparison bounds and their relaxations

Outer bounds on the effective strength domain (2.3) are obtained here by means of the linear-comparison method recently developed by Idiart & Ponte Castañeda (2007*a,b*). The main idea behind this method is to introduce a heterogeneous comparison solid with a linear stress–strain rate local response characterized by a positive-semidefinite,¹ symmetric compliance tensor field $\mathbb{S}(\mathbf{x})$ and, by making

¹Positive-semi definiteness of a fourth-order tensor \mathbb{S} will be indicated by the inequality $\mathbb{S} \geq 0$.

judicious use of the Legendre transform, to rewrite the domain (2.3) as

$$\tilde{P} = \{ \bar{\boldsymbol{\sigma}} : \tilde{u}_0(\bar{\boldsymbol{\sigma}}; \mathbb{S}(\mathbf{x})) \leq v(\mathbb{S}(\mathbf{x})), \forall \mathbb{S}(\mathbf{x}) \geq 0 \}, \tag{3.1}$$

where

$$\tilde{u}_0(\bar{\boldsymbol{\sigma}}; \mathbb{S}(\mathbf{x})) = \min_{\boldsymbol{\sigma} \in \mathcal{S}(\bar{\boldsymbol{\sigma}})} \left\langle \frac{1}{2} \boldsymbol{\sigma} \cdot \mathbb{S}(\mathbf{x}) \boldsymbol{\sigma} \right\rangle \quad \text{and} \quad v(\mathbb{S}(\mathbf{x})) = \sum_{r=1}^N c^{(r)} \langle v^{(r)}(\mathbb{S}(\mathbf{x})) \rangle^{(r)}. \tag{3.2}$$

In these expressions, \tilde{u}_0 represents the effective stress potential of the heterogeneous linear-comparison solid, while the functions $v^{(r)}$, defined as

$$v^{(r)}(\mathbb{S}) = \sup_{\boldsymbol{\sigma} \in P^{(r)}} \frac{1}{2} \boldsymbol{\sigma} \cdot \mathbb{S} \boldsymbol{\sigma}, \tag{3.3}$$

represent a measure of the nonlinearity of the local stress–strain rate plastic relation. Note that the compliance field $\mathbb{S}(\mathbf{x})$ is dictated by the representation (3.1) itself. The reader is referred to the work of Idiart & Ponte Castañeda (2007a, §4b) for details on the derivation.

Any restriction on the compliance field $\mathbb{S}(\mathbf{x})$ in (3.1) generates a set containing \tilde{P} and, therefore, can be used to generate outer bounds on the effective yield surface of the polycrystalline aggregate. If the compliance field $\mathbb{S}(\mathbf{x})$ is restricted to constant-per-phase fields of the form

$$\mathbb{S}(\mathbf{x}) = \sum_{r=1}^N \chi^{(r)}(\mathbf{x}) \mathbb{S}^{(r)} \quad \text{with} \quad \mathbb{S}^{(r)} \geq 0, \tag{3.4}$$

the heterogeneous comparison solid becomes a linear polycrystal with the same microgeometry as the nonlinear polycrystal, and the following enlarged strength domain is obtained (Idiart & Ponte Castañeda 2007a):

$$\tilde{P} \subset \tilde{P}_+ = \{ \bar{\boldsymbol{\sigma}} : \tilde{u}_0(\bar{\boldsymbol{\sigma}}; \mathbb{S}^{(s)}) \leq v(\mathbb{S}^{(s)}), \forall \mathbb{S}^{(r)} \geq 0 \}, \tag{3.5}$$

where

$$\tilde{u}_0(\bar{\boldsymbol{\sigma}}; \mathbb{S}^{(s)}) = \min_{\boldsymbol{\sigma} \in \mathcal{S}(\bar{\boldsymbol{\sigma}})} \sum_{r=1}^N c^{(r)} \left\langle \frac{1}{2} \boldsymbol{\sigma} \cdot \mathbb{S}^{(r)} \boldsymbol{\sigma} \right\rangle^{(r)} \quad \text{and} \quad v(\mathbb{S}^{(s)}) = \sum_{r=1}^N c^{(r)} v^{(r)}(\mathbb{S}^{(r)}). \tag{3.6}$$

Note that the functions $v^{(r)}$ are now uniform. The boundary of \tilde{P}_+ is given by

$$\partial \tilde{P}_+ = \left\{ \bar{\boldsymbol{\sigma}} : \sup_{\mathbb{S}^{(r)} \geq 0} [\tilde{u}_0(\bar{\boldsymbol{\sigma}}; \mathbb{S}^{(s)}) - v(\mathbb{S}^{(s)})] = 0 \right\}, \tag{3.7}$$

and represents a surface in the space of macroscopic stresses that bounds from outside the effective yield surface of the polycrystalline solid. It can be shown that the optimization with respect to the compliance tensors $\mathbb{S}^{(r)}$ is concave. A dual version of this bound in terms of support functions was proposed earlier by Olson (1994); when the phases are isotropic, the bound (3.7) reduces to the bound initially derived by Ponte Castañeda (1991).

An alternative form of (3.7) can be derived by exploiting the fact that the functions \tilde{u}_0 and v are homogeneous of degree one in the tensors $\mathbb{S}^{(r)}$ (see Idiart & Ponte Castañeda 2007a); the result is

$$\partial\tilde{P}_+ = \left\{ \bar{\boldsymbol{\sigma}} : \bar{\boldsymbol{\sigma}} = \lambda \bar{\boldsymbol{\Sigma}} \text{ with } \|\bar{\boldsymbol{\Sigma}}\| = 1 \text{ and } \lambda = \left(\sup_{\mathbb{S}^{(r)} \geq 0} \frac{\tilde{u}_0(\bar{\boldsymbol{\Sigma}}; \mathbb{S}^{(s)})}{v(\mathbb{S}^{(s)})} \right)^{-1/2} \right\}, \quad (3.8)$$

where $\|\cdot\|$ denotes the Euclidean norm of a tensor. This form is preferred over (3.7) from a computational standpoint, since it allows the construction of the effective yield surface by computing a scalar factor λ for specified directions $\bar{\boldsymbol{\Sigma}}$ in stress space without having to solve a nonlinear equation as in (3.7). The optimization problem in (3.8) is, however, non-concave.

To compute the outer bound (3.8) we must determine the effective stress potential \tilde{u}_0 of a linear polycrystal with the same microgeometry as the original polycrystal and with phase compliance tensors $\mathbb{S}^{(r)}$. Note that, in general, the tensors $\mathbb{S}^{(r)}$ ($r = 1, \dots, N$) do not correspond to rotations of a reference compliance tensor; thus, the linear-comparison polycrystal is not monolithic as the nonlinear polycrystal. In view of the local linearity, this potential can be written as

$$\tilde{u}_0(\bar{\boldsymbol{\sigma}}; \mathbb{S}^{(s)}) = \frac{1}{2} \bar{\boldsymbol{\sigma}} \cdot \tilde{\mathbb{S}}(\mathbb{S}^{(s)}) \bar{\boldsymbol{\sigma}}, \quad (3.9)$$

where $\tilde{\mathbb{S}}$ is the effective compliance tensor of the linear-comparison polycrystal. In practice, the tensor $\tilde{\mathbb{S}}$ cannot be computed and it must be bounded from below—in the sense of quadratic forms—so that the set (3.8) still bounds from the outside the effective yield surface of the polycrystals.² The results reported in this work make use of the lower bounds of Willis (1977, 1982), given by

$$\tilde{\mathbb{S}} = \left[\sum_{r=1}^N c^{(r)} (\mathbb{S}^{(r)} + \mathbb{S}^*)^{-1} \right]^{-1} - \mathbb{S}^*, \quad (3.10)$$

where $\mathbb{S}^* = \mathbb{Q}_0^{-1} - \mathbb{S}_0$ is the constraint tensor introduced by Hill (1965), \mathbb{S}_0 is a reference compliance tensor, and \mathbb{Q}_0 is a microstructural tensor that depends on \mathbb{S}_0 and on the ‘shape’ of the two-point correlation functions $p^{(rs)}(\mathbf{x}, \mathbf{x}')$ for the distribution of the grain orientations within the aggregate—the reader is referred to Willis (1977, 1982) for details. Thus, these bounds depend on one- and two-point microstructural statistics, and are sharper than the corresponding elementary bound. The appropriate choice of \mathbb{S}_0 depends on the particular class of polycrystals under consideration.

In order to generate a lower bound for the *full* class of polycrystals with prescribed one- and two-point statistics, the reference compliance tensor \mathbb{S}_0 must

²If an upper bound is used instead, the surface (3.8) ceases to be an outer bound on the effective yield surface and becomes an estimate. As it stands, the linear-comparison method employed in this work cannot produce inner bounds on the effective yield surface. A strategy to produce inner rather than outer bounds is available from the works of Willis (1994) and Talbot & Willis (1998), but no attempts have been made yet to compute such bounds in the context of polycrystalline plastic solids under general loading conditions.

be chosen so that the inequality $\mathbb{S}^{(r)} - \mathbb{S}_0 \geq 0$ holds for all r . Noting that the tensors $\mathbb{S}^{(r)}$ are incompressible—see further below—a simple choice is

$$\mathbb{S}_0 = \frac{1}{2\mu_0} \mathbb{K}, \tag{3.11}$$

where \mathbb{K} is the standard fourth-order incompressible identity tensor and $(2\mu_0)^{-1}$ is taken to be the smallest eigenvalue of all the tensors $\mathbb{S}^{(r)}$. The resulting bound (3.10) for $\tilde{\mathbb{S}}$ is commonly referred to as the Hashin–Shtrikman lower bound, and the resulting surface (3.8) bounds from the outside the strength domain of all polycrystals with prescribed one- and two-point statistics.

The result (3.10) also serves to generate bounds for *subclasses* of polycrystals with prescribed statistics. For instance, by choosing

$$\mathbb{S}_0 = \tilde{\mathbb{S}} \tag{3.12}$$

the resulting $\tilde{\mathbb{S}}$ reproduces exactly the so-called self-consistent estimate. This estimate is known to be particularly accurate for polycrystalline solids such as the ones considered in this work—see Willis (1982) and Lebensohn *et al.* (2004)—but more importantly, it is known to be exact for a special subclass of polycrystals with prescribed one- and two-point statistics, consisting of hierarchical microstructures with widely separated length scales. Therefore, the resulting surface (3.8) bounds from the outside the strength domain of all polycrystals belonging to that particular subclass—see Nebozhyn *et al.* (2001).

In turn, the computation of the functions $v^{(r)}$ in v requires the solution of the optimization problem (3.3). Since the $P^{(r)}$ are closed convex sets, this optimization problem amounts to finding the maximum of a convex function relative to a convex set. It is known from convex analysis—see Rockafellar (1970)—that the maximum in (3.3) is attained at one or more of the extreme points of the set $P^{(r)}$. For the crystalline solids considered in this work, the sets $P^{(r)}$ are convex polyhedra formed by the set of planes (or facets) whose equations are given by the equalities in (2.1), and the extreme points are the vertices of those polyhedra. We denote the set of V vertices of $P^{(r)}$ as

$$\hat{P}^{(r)} = \left\{ \hat{\boldsymbol{\sigma}}_{(v)}^{(r)}, v = 1, \dots, V \right\}. \tag{3.13}$$

The tensors $\hat{\boldsymbol{\sigma}}_{(v)}^{(r)}$ are related to corresponding tensors $\hat{\boldsymbol{\sigma}}_{(v)}$ for the ‘reference’ crystal via $\hat{\boldsymbol{\sigma}}_{(v)}^{(r)} = \mathbf{Q}^{(r)\text{T}} \hat{\boldsymbol{\sigma}}_{(v)} \mathbf{Q}^{(r)}$. Vertex sets for common crystal symmetries have been determined by Kocks *et al.* (1983), Tomé & Kocks (1985) and Orleans-Joliet *et al.* (1988), among others, as it is required in applications of the classical Taylor theory of polycrystalline plasticity. More generally, however, vertex enumeration algorithms must be employed—see appendix A—to determine the sets $\hat{P}^{(r)}$. In any event, the optimization problem (3.3) reduces to finding the maximum of a convex function over the (finite) vertex set $\hat{P}^{(r)}$:

$$v^{(r)}(\mathbb{S}^{(r)}) = \max_{v=1, \dots, V} \left\{ \frac{1}{2} \hat{\boldsymbol{\sigma}}_{(v)}^{(r)} \cdot \mathbb{S}^{(r)} \hat{\boldsymbol{\sigma}}_{(v)}^{(r)} \right\}, \tag{3.14}$$

a function that is very easy to evaluate. Note, however, that this max-function is a non-smooth function of $\mathbb{S}^{(r)}$.

Finally, the optimization with respect to the compliance tensors $\mathbb{S}^{(r)}$ in (3.8) must be solved. Owing to the insensitivity of the strength domains $P^{(r)}$ on hydrostatic stress, the optimal compliance tensors $\mathbb{S}^{(r)}$ are incompressible. Thus, each $\mathbb{S}^{(r)}$ requires 15 parameters—or components—to be fully specified, so that the bound (3.8) requires the solution of a constrained optimization problem of a non-concave, non-smooth objective function with respect to $15 \times N$ variables. The fact that the objective function has multiple wells—as is numerically observed—adds to the computational complexity. A solution strategy is described in appendix A. It is possible, however, to simplify the optimization problem at the expense of relaxing the bound as described next.

(a) *Relaxed bounds \tilde{P}'_+*

The computation of the bound (3.8) can be simplified by restricting further the set of compliance tensors $\mathbb{S}^{(r)}$ to those of the form

$$\mathbb{S}^{(r)} = 2 \sum_{k=1}^K \alpha_{(k)}^{(r)} \boldsymbol{\mu}_{(k)}^{(r)} \otimes \boldsymbol{\mu}_{(k)}^{(r)}, \quad \alpha_{(k)}^{(r)} \geq 0, \tag{3.15}$$

where the $\boldsymbol{\mu}_{(k)}^{(r)}$ are the Schmid tensors of the crystalline phase r and the scalar variables $\alpha_{(k)}^{(r)}$ represent slip compliances. This class of compliance tensors arise naturally in the linear-comparison bounds of deBotton & Ponte Castañeda (1995). With this restriction, the functions $v^{(r)}$ take the form

$$\begin{aligned} v^{(r)}(\mathbb{S}^{(r)}) &= \max_{v=1, \dots, V} \left\{ \sum_{k=1}^K \alpha_{(k)}^{(r)} (\hat{\boldsymbol{\sigma}}_{(v)}^{(r)} \cdot \boldsymbol{\mu}_{(k)}^{(r)})^2 \right\} \\ &= \max_{v=1, \dots, V} \left\{ \sum_{k=1}^K \alpha_{(k)}^{(r)} (\hat{\boldsymbol{\sigma}}_{(v)} \cdot \boldsymbol{\mu}_{(k)})^2 \right\} \doteq v^{(r)'}(\alpha_{(k)}^{(r)}), \end{aligned} \tag{3.16}$$

where the products $\hat{\boldsymbol{\sigma}}_{(v)} \cdot \boldsymbol{\mu}_{(k)}$ are independent of crystal orientation and must be computed just once. The yield surface (3.8) is then bounded from the outside by the surface

$$\partial \tilde{P}'_+ = \left\{ \bar{\boldsymbol{\sigma}} : \bar{\boldsymbol{\sigma}} = \Lambda \bar{\boldsymbol{\Sigma}} \text{ with } \|\bar{\boldsymbol{\Sigma}}\| = 1 \text{ and } \Lambda = \left(\sup_{\alpha_{(k)}^{(s)} \geq 0} \frac{\tilde{u}_0(\bar{\boldsymbol{\Sigma}}; \alpha_{(k)}^{(s)})}{v'(\alpha_{(k)}^{(s)})} \right)^{-1/2} \right\}, \tag{3.17}$$

where v' is defined in terms of the functions $v^{(r)'}$ by an expression analogous to (3.6). This relaxed bound requires the solution of a constrained optimization problem of a non-concave, non-smooth function with respect to $K \times N$ variables.³ However, unlike the bound (3.8), the bound (3.17) involves a single-well objective function—as is numerically observed—thus simplifying computations significantly.

³Owing to the homogeneity of degree zero of the objective function in the slip compliances $\alpha_{(k)}^{(r)}$, the number of independent variables can be reduced to $K \times N - 1$.

(b) Fully relaxed bounds \tilde{P}''_+

In addition to the restriction (3.15), further simplification results from relaxing the optimization problem in the functions $v^{(r)}$ by making use of the inequality

$$\begin{aligned}
 v^{(r)}(\mathbb{S}^{(r)}) &= \sup_{\boldsymbol{\sigma} \in P^{(r)}} \frac{1}{2} \boldsymbol{\sigma} \cdot \mathbb{S}^{(r)} \boldsymbol{\sigma} = \sup_{\boldsymbol{\sigma} \in P^{(r)}} \sum_{k=1}^K \alpha_{(k)}^{(r)} (\boldsymbol{\sigma} \cdot \boldsymbol{\mu}_{(k)}^{(r)})^2 \\
 &\leq \sum_{k=1}^K \alpha_{(k)}^{(r)} \sup_{\boldsymbol{\sigma} \in P^{(r)}} (\boldsymbol{\sigma} \cdot \boldsymbol{\mu}_{(k)}^{(r)})^2 = \sum_{k=1}^K \alpha_{(k)}^{(r)} (\boldsymbol{\tau}_0^{(k)})^2 \doteq v^{(r)''}(\alpha_{(k)}^{(r)}). \tag{3.18}
 \end{aligned}$$

In view of this inequality, the surface

$$\partial \tilde{P}''_+ = \left\{ \bar{\boldsymbol{\sigma}} : \bar{\boldsymbol{\sigma}} = \mathcal{A} \bar{\boldsymbol{\Sigma}} \text{ with } \|\bar{\boldsymbol{\Sigma}}\| = 1 \text{ and } \mathcal{A} = \left(\sup_{\alpha_{(k)}^{(r)} > 0} \frac{\tilde{u}_0(\bar{\boldsymbol{\Sigma}}; \mathbb{S}^{(r)})}{v''(\alpha_{(k)}^{(s)})} \right)^{-1/2} \right\}, \tag{3.19}$$

where the function v'' is defined in terms of the functions $v^{(r)''}$ by an expression analogous to (3.6), bounds from the outside the surface $\partial \tilde{P}''_+$ given by (3.17). This fully relaxed bound agrees exactly with the bound originally derived—following a different route—by deBotton & Ponte Castañeda (1995). As the relaxed bound (3.17), it requires the solution of a constrained optimization problem of a non-concave function with respect to $K \times N$ variables. However, the objective function has a single-well structure—observed numerically—and, unlike the functions $v^{(r)}$ and $v^{(r)'}$, the functions $v^{(r)''}$ are explicit and smooth, which simplifies the computations further. Note, however, that the inequality in (3.18) becomes an equality when the total number of slip systems at the single-crystal level is five and all of them are linearly independent. In that case, the bounds (3.17) and (3.19) coincide.

4. Results for cubic and hexagonal polycrystals

The above linear-comparison bounds are applied here to various classes of polycrystalline solids in order to explore the effect of crystal anisotropy on the macroscopic plastic strength. In all cases, both crystallographic and morphological textures are assumed to be *statistically isotropic*, so that the aggregate exhibits overall plastic isotropy. This amounts to assuming that the two-point correlation functions $p^{(rs)}$ are isotropic and that $c^{(r)} = 1/N$ ($r = 1, \dots, N$) in (3.10). In view of the overall isotropy, the effective yield surface can be expressed as

$$\partial \tilde{P} = \{ \bar{\boldsymbol{\sigma}} : \bar{\sigma}_e - \tilde{\sigma}_0(\bar{\theta}) = 0 \}, \tag{4.1}$$

where $\tilde{\sigma}_0$ is an *effective flow stress*, and $\bar{\sigma}_e$ and $\bar{\theta}$ are stress invariants of the macroscopic deviatoric stress $\bar{\boldsymbol{\sigma}}_d$ defined by

$$\bar{\sigma}_e = \sqrt{\frac{3}{2} \bar{\boldsymbol{\sigma}}_d \cdot \bar{\boldsymbol{\sigma}}_d} \quad \text{and} \quad \cos(3\bar{\theta}) = \frac{27}{2} \det \left(\frac{\bar{\boldsymbol{\sigma}}_d}{\bar{\sigma}_e} \right). \tag{4.2}$$

Thus, the effective yield surface is completely characterized by the effective flow stress, which depends on the stress invariant $\bar{\theta}$ and on the properties of the crystals composing the aggregate. The stress invariant $\bar{\theta}$ is a homogeneous function of degree zero in $\bar{\sigma}$ and characterizes the ‘direction’ of the macroscopic stress in deviatoric space: the particular values $\bar{\theta} = 0$ and $\bar{\theta} = \pi/6$ correspond to uniaxial tension and simple shear loadings, respectively. However, the variation of $\tilde{\sigma}_0$ with $\bar{\theta}$ is known to be small—see, for instance, Nebozhyn *et al.* (2001)—and will not be studied further here; only the case of *uniaxial tension* is considered. Note that an outer bound on $\partial\tilde{P}$ induces an *upper* bound on $\tilde{\sigma}_0$.

The results presented below correspond to 200 crystal orientations ($N = 200$) prescribed according to a Sobol sequence Sobol (1967) in order to generate textures as close as possible to isotropy—see Lebensohn *et al.* (2011). In any event, the exact same set of orientations were used for all computations so that comparisons between the different bounds are meaningful. It is emphasized that, owing to the multi-well structure of the relevant objective function, the non-relaxed bounds presented below need not be optimal: a particular well is effectively selected in the optimization process by identifying the initial guess for the compliance tensors $\mathbb{S}^{(r)}$ with the optimal compliance tensors of the corresponding relaxed bounds. This and other numerical aspects of the calculations are discussed in appendix A.

Henceforth, non-relaxed bounds of the Hashin–Shtrikman and self-consistent types are labelled HS and SC, respectively, and their relaxed and fully relaxed versions are denoted by primed and double-primed labels.

(a) Cubic polycrystals

Results are reported here for polycrystalline solids with three types of cubic crystals: face-centred cubic (FCC), body-centred cubic (BCC) and ionic crystals.

In FCC crystals, the plastic deformation takes place on a set of four slip planes of the type $\{111\}$ along three slip directions (per plane) of type $\langle 110 \rangle$, which constitute a set of 12 slip systems ($K = 12$). Of these, five are linearly independent, allowing arbitrary plastic deformation of the grains—see, for example, Groves & Kelly (1963). The 12 systems define a yield surface with 56 vertices ($V = 56$). The yield surface geometry of FCC crystals has been described in detail by Kocks *et al.* (1983).

In BCC crystals, the plastic deformation is assumed to be accommodated through slip along the $\langle 111 \rangle$ directions and to occur on the $\{110\}$ and $\{112\}$ planes—pencil glide along $\{123\}$ planes is not considered—which constitute a set of 24 slip systems ($K = 24$). Of these, five are linearly independent. The 24 systems define a yield surface with 432 vertices ($V = 432$). The yield surface geometry of BCC crystals has been described in detail by Orlans-Joliet *et al.* (1988).

In ionic crystals, the plastic deformation is assumed to take place on three different families of slip systems: $\{110\}\langle 110 \rangle$, $\{100\}\langle 110 \rangle$, $\{111\}\langle 110 \rangle$. They will be referred to as *A*, *B* and *C* families, having flow stresses τ_A , τ_B and τ_C , respectively. The *A* family consists of six systems, among which two are linearly independent and can accommodate only normal components of strain rate—relative to the cubic axes of the crystal. The *B* family consists of six systems, among which

Table 1. Bounds on the effective flow stress $\tilde{\sigma}_0$ of isotropic polycrystals with low-anisotropy crystals (FCC, BCC, IONIC) under uniaxial tension. The results are normalized by the slip flow stress τ_0 .

	Taylor	HS''	HS'	HS	SC''	SC'	SC	Reuss
FCC	3.07	3.06	3.05	3.05	2.95	2.92	2.91	2.00
BCC	2.80	2.80	2.79	2.79	2.75	2.66	2.65	2.00
IONIC	2.40	2.40	2.40	2.40	2.37	2.36	2.35	2.00

three are linearly independent and can only accommodate shear components of strain rate—relative to the cubic axes of the crystal. Because of the orthogonality of the A and B systems, the two families together provide five independent slip systems so that a general isochoric deformation can be accommodated. The C family, in turn, consists of the same 12 slip systems of an FCC crystal. Thus, the three families together consist of 24 slip systems ($K = 24$), which define a yield surface with 312 vertices ($V = 312$).

Table 1 reports the various bounds for the macroscopic uniaxial strength $\tilde{\sigma}_0$ of low-anisotropy FCC, BCC and ionic solids with all slip systems having the same flow stress $\tau_0^{(k)} = \tau_0 (k = 1, \dots, K)$. Results are normalized by τ_0 . We begin by noting that the numerical values for the elementary and fully relaxed linear-comparison bounds are consistent with previously reported values—cf. Nebozhyn *et al.* (2001) and Liu & Ponte Castañeda (2004). Note that, in particular, the Reuss bound is insensitive to crystal anisotropy. The main observation in the context of these results, however, is that the non-relaxed bounds of the HS and SC type improve, albeit slightly, on their relaxed counterparts in all cases except the IONIC-HS case. The improvement is seen to be more noticeable in the SC results, with the largest improvement amounting to about 4 per cent in the case of BCC solids. On the other hand, all HS bounds are found to lie very close to the Taylor upper bound, in agreement with earlier results—see Liu & Ponte Castañeda (2004). The fact that even the new non-relaxed bounds of the HS type remain so close to the Taylor bounds supports the view that this feature should be attributed to the possibly non-optimal character of the linear Hashin–Shtrikman bounds for polycrystals rather than to the linearization scheme of the linear-comparison procedure. Finally, it is observed that the second relaxation is responsible for most of the difference between the non-relaxed and fully relaxed bounds. In fact, this is observed for all the other material types considered below. For that reason, the relaxed bounds are omitted henceforth and only comparisons between the non-relaxed and the fully relaxed bounds are reported.

Figure 1 shows the various bounds for high-anisotropy ionic solids in the absence of C-type slip ($\tau_C = \infty$). Figure 1a displays plots for $\tilde{\sigma}_0$, normalized by τ_A , as a function of increasing slip contrast $\tau_B/\tau_A \geq 1$, while figure 1b displays plots for $\tilde{\sigma}_0$, normalized by τ_B , as a function of increasing slip contrast $\tau_A/\tau_B \geq 1$. We begin by noting that the elementary bounds diverge as the crystal anisotropy increases: the Taylor bound grows linearly with slip contrast, while the Reuss bound remains constant. The HS and SC results lie between these bounds, as they should. Once again, the non-relaxed bounds are found to improve on their fully relaxed counterparts. In the case of the HS bounds, the improvement is

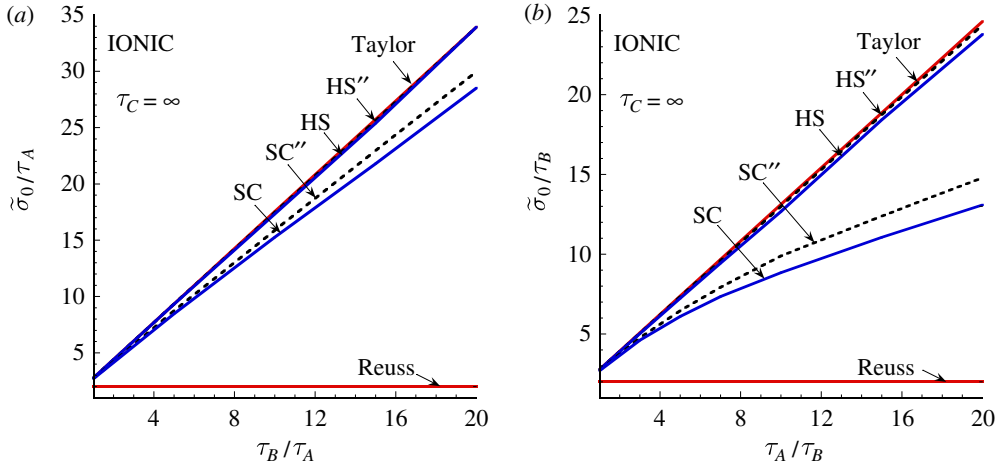


Figure 1. Bounds on the effective flow stress $\tilde{\sigma}_0$ of isotropic polycrystals with highly anisotropic ionic crystals under uniaxial tension as a function of slip contrast. (Online version in colour.)

modest and all results lie very close to the Taylor bound for the entire range of plastic anisotropies considered. In the case of the SC bounds, by contrast, the results diverge from the Taylor bound and the difference between the SC and SC'' bounds becomes appreciable as slip contrast increases. The largest differences are found to be about 5 per cent as *A*-type slip becomes dominant—see figure 1*a*—and 13 per cent as *B*-type slip becomes dominant—see figure 1*b*. These results suggest that even though the relaxation (3.18) on the function *v* deteriorates with increasing number of crystal slip systems, the deviation between the non-relaxed and the fully relaxed bounds depends more strongly on crystal anisotropy.

(b) Hexagonal polycrystals

Results are reported here for polycrystalline solids with hexagonal crystal symmetry with ratio $c/a = 1.59$. Plastic deformation is assumed to take place on three sets of slip systems: three basal systems $\{0001\}\langle 11\bar{2}0 \rangle$, three prismatic systems $\{10\bar{1}0\}\langle 11\bar{2}0 \rangle$ and 12 first-order pyramidal- $\langle c + a \rangle$ systems $\{10\bar{1}\bar{1}\}\langle 11\bar{2}3 \rangle$. They will be referred to as *A*, *B* and *C* families, having flow stresses τ_A , τ_B and τ_C , respectively. Note that the three basal plus the three prismatic systems supply only four linearly independent systems, allowing no straining along the hexagonal crystal axis. On the other hand, the 12 pyramidal systems contain a set of five independent systems. The three families together provide a set of 18 slip systems ($K = 18$) which define a yield surface with 242 vertices ($V = 242$). The yield surface geometry of HCP crystals with prismatic and pyramidal systems has been described in detail by Tomé & Kocks (1985).

Figure 2 shows the various bounds for high-anisotropy HCP solids. Figure 2*a* displays plots for $\tilde{\sigma}_0$, normalized by τ_A , for the choice $\tau_C = \tau_B$, as a function of increasing slip contrast $\tau_B/\tau_A \geq 1$, while figure 2*b* displays plots for the same quantity for the choice $\tau_B = \tau_A$, as a function of increasing slip contrast $\tau_C/\tau_A \geq 1$. As in the case of ionic polycrystals, the Taylor and Reuss bounds are seen to

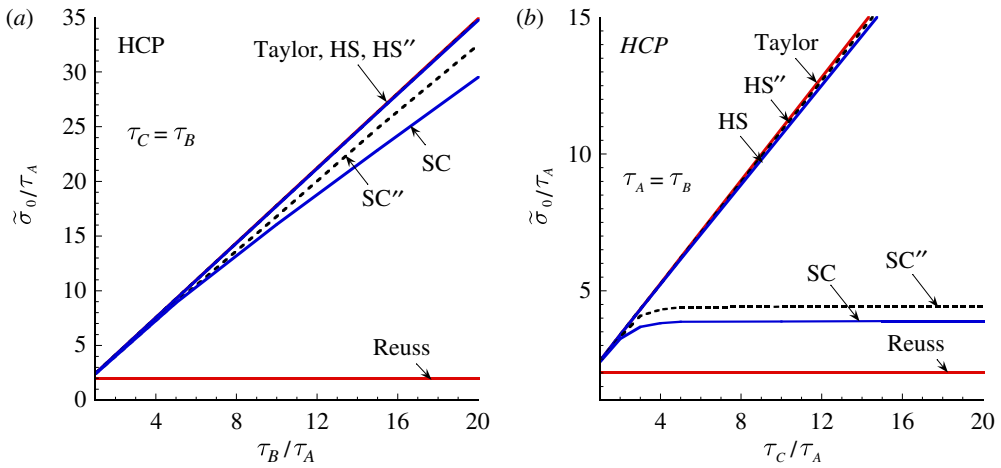


Figure 2. Bounds on the effective flow stress $\tilde{\sigma}_0$ of isotropic polycrystals with highly anisotropic HCP crystals under uniaxial tension as a function of slip contrast. (Online version in colour.)

diverge as the crystal anisotropy increases, with the Taylor bound growing linearly with slip contrast and the Reuss bound remaining constant. Once again, the non-relaxed bounds are found to improve on elementary bounds and on their fully relaxed counterparts in all cases considered, the improvement being very modest for the HS results and more noticeable for the SC results. The largest improvements observed in the SC results are about 10 per cent when basal slip becomes dominant—see figure 2a—and exceed 13 per cent as pyramidal slip vanishes—see figure 2b. These results thus confirm that the deviation between the non-relaxed and fully relaxed bounds depends more critically on crystal anisotropy than on the number of crystal slip systems. It should be mentioned, however, that this difference does not increase monotonically with slip contrast. For instance, non-relaxed and fully relaxed SC bounds have been calculated for hexagonal polycrystals with $\tau_B = 2\tau_A$ and $\tau_C = 20\tau_A$, and have been found to be, respectively, $\tilde{\sigma}_0 = 5.82\tau_A$ and $\tilde{\sigma}_0 = 6.70\tau_A$, which differ by more than 15 per cent.

(c) Polycrystals with deficient slip systems

As the slip contrasts in figures 1 and 2 tend to infinity, the number of linearly independent slip systems in the corresponding constituent crystals becomes deficient, i.e. less than five. In this limit, the various bounds for the effective flow stress follow a scaling law of the form $\tilde{\sigma}_0 \sim M^\gamma$, where M is the relevant slip contrast. For the Taylor and HS bounds $\gamma = 1$, and for the Reuss bound $\gamma = 0$, independently of crystal symmetry. By contrast, the exponent γ associated with SC bounds does depend on crystal symmetry. Nebozhyn *et al.* (2001) have shown that for the fully relaxed SC bounds $\gamma = (4 - J)/2$, where J is the number of independent slip systems left in the limit $M \rightarrow \infty$. According to this law, single crystals with four independent systems still allow the polycrystal to accommodate any macroscopic deformation, but single crystals with three or less independent systems do not. Both the non-relaxed and fully relaxed SC

results provided in figures 1 and 2 are entirely consistent with this scaling law.⁴ Indeed, the SC bounds shown in figure 1*a* for dominant *A*-type slip ($J = 2$) and in figure 1*b* for dominant *B*-type slip ($J = 3$) are consistent with exponents $\gamma = 1$ and $\gamma = 1/2$, respectively, while the SC bounds shown in figure 2*a* for dominant basal slip ($J = 2$) and in figure 2*b* for dominant basal + prismatic slip ($J = 4$) are consistent with exponents $\gamma = 1$ and $\gamma = 0$, respectively. Thus, the scaling law is preserved by the relaxation of the function v in the linear-comparison method. The differences between the non-relaxed and fully relaxed SC bounds for these extremely low-symmetry solids remain in the order of those already reported above.

5. Concluding remarks

The results presented in this work have demonstrated the capability of the non-relaxed linear-comparison bounds of Idiart & Ponte Castañeda (2007*a*) to improve on the relaxed bounds of deBotton & Ponte Castañeda (1995) when applied to polycrystalline plastic solids with a wide range of single-crystal plastic anisotropies. While scanty in the case of Hashin–Shtrikman results, the improvement in the case of self-consistent results can exceed 15 per cent for certain low-symmetry hexagonal polycrystals. These are the sharpest bounds available to date for polycrystalline plastic solids with prescribed one- and two-point microstructural statistics.

Interestingly, despite the fact that the relaxation introduced by deBotton & Ponte Castañeda (1995) on the function v deteriorates with increasing number of slip systems, the larger improvements were observed in the context of cubic and hexagonal polycrystals with deficient slip systems. Given that these are materials with a strong heterogeneity contrast, the question arises as to whether larger differences between the non-relaxed and relaxed linear-comparison bounds will appear in the context of (two-phase) polycrystalline voided solids where the overall heterogeneity contrast is infinitely strong. Such bounds would help current efforts directed towards developing micromechanical models for voided polycrystals to incorporate texture effects in ductile-failure theories of engineering alloys—see Lebensohn *et al.* (2011)—calculations are now underway and will be reported upon completion.

We conclude by noting that the linear-comparison method employed in this work was originally derived in the more general context of viscoplasticity, which includes rigid–perfectly plasticity as a limiting case. In that context, the function v requires the solution of a non-concave optimization problem over a continuous set, which cannot be reduced to a maximization over a finite set as in the rigid–perfectly plastic case, and thus calls for special numerical treatment—see Idiart & Ponte Castañeda (2007*b*). However, many materials often exhibit very low strain–rate sensitivity, and in that case, the rigid–perfectly plastic solutions generated in this work should provide sufficiently accurate initial guesses in the linear-comparison procedure to compute the function v by means of conventional concave optimization algorithms.

⁴The trends have been verified by unpublished results for $M = 100$.

This work was partially supported by the Agencia Nacional de Promoción Científica y Tecnológica (Argentina) through Grant PICT-2008-0226. Thanks are due to F. A. Bacchi (Universidad Nacional de La Plata, Argentina) for assisting with the use of the GFC computer cluster, and to R. A. Lebensohn (Los Alamos National Laboratory, USA) for providing the Sobol sequences used to represent isotropic textures.

Appendix A. Numerical aspects of the calculations

(a) Vertex tensors $\hat{\sigma}_{(v)}$

The functions $v^{(r)}$ and $v^{(r)'}$ as defined by (3.14) and (3.16) require knowledge of the vertex tensors $\hat{\sigma}_{(v)}$. These are the vertices of a closed polyhedron in five-dimensional stress space whose facets are the $2K$ planes defined by $\boldsymbol{\sigma} \cdot \boldsymbol{\mu}_{(k)} = \pm \tau_0^{(k)}$ ($k = 1, \dots, K$). To determine the entire set of vertices for a given type of crystal, a vertex enumeration algorithm must be employed. A popular algorithm for vertex enumeration of polyhedra is available from the work of Avis & Fukuda (1992). However, we found more reliable to employ a related algorithm recently developed by Terzer (2009) to enumerate extreme rays of multi-dimensional polyhedral cones. In this approach, one constructs a six-dimensional polyhedral cone whose cross section at a given distance from the apex conforms to the five-dimensional polyhedral yield surface of the single crystal. The intersection between the extreme rays of the cone and that particular cross section gives all vertices of the yield surface.

(b) Effective compliance tensor $\tilde{\mathbb{S}}$

The effective stress potential \tilde{u}_0 as given by (3.9) requires the computation of the effective compliance tensor $\tilde{\mathbb{S}}$ as given by (3.10) for the case of statistically isotropic texture.

For the choice (3.11), $\mathbb{Q}_0 = 4\mu_0\mathbb{J} + (6\mu_0/5)\mathbb{K}$ —see Willis (1982)—and the expression (3.10) for $\tilde{\mathbb{S}}$ is explicit. Here, \mathbb{J} and \mathbb{K} are the standard fourth-order, isotropic, shear and hydrostatic projection tensors, respectively.

For the choice (3.12), the tensor \mathbb{Q}_0 depends on $\tilde{\mathbb{S}}$ and the expression (3.10) for $\tilde{\mathbb{S}}$ is implicit. In the case of uniaxial tension, the tensor $\tilde{\mathbb{S}}$ exhibits transverse isotropy about the tensile axis, and the tensor \mathbb{Q}_0 in terms of $\tilde{\mathbb{S}}$ can be found, for instance, in Willis (1982). The resulting equation (3.10) can be easily solved for $\tilde{\mathbb{S}}$ by the fixed-point method.

(c) Optimization procedure

The constrained optimization with respect to positive-semidefinite, symmetric compliance tensors $\mathbb{S}^{(r)}$ in the bound (3.8) was rewritten as an unconstrained optimization with respect to symmetric fourth-order tensors $\mathbb{A}^{(r)}$ such that $\mathbb{S}^{(r)} = \mathbb{A}^{(r)}\mathbb{A}^{(r)}$. By the same token, the constrained optimization with respect to the positive slip compliances $\alpha_{(k)}^{(r)}$ in the bounds (3.17) and (3.19) was rewritten as an unconstrained optimization with respect to scalar variables $a_{(k)}^{(r)}$ such

that $\alpha_{(k)}^{(r)} = (a_{(k)}^{(r)})^2$. The objective functions were then optimized by making use of Brent's algorithm (Brent 2002) for minimization without derivatives. This algorithm requires an initial guess for the optimizing variables. The following sequence was followed:

- compute fully relaxed bounds
 - (i) with $\tilde{\mathbb{S}}$ given by the Taylor bound and the initial guess given by $\alpha_{(k)}^{(r)} = (\tau_0^{(k)})^{-1}$;
 - (ii) with $\tilde{\mathbb{S}}$ given by the Hashin–Shtrikman bound and the initial guess given by the optimal $\alpha_{(k)}^{(r)}$ of the previous step; and
 - (iii) with $\tilde{\mathbb{S}}$ given by the self-consistent bound and the initial guess given by the optimal $\alpha_{(k)}^{(r)}$ of the previous step;
- compute relaxed bounds
 - (i) with $\tilde{\mathbb{S}}$ given by the Hashin–Shtrikman bound and the initial guess given by the optimal $\alpha_{(k)}^{(r)}$ of the step 1.2 and
 - (ii) with $\tilde{\mathbb{S}}$ given by the self-consistent bound and the initial guess given by the optimal $\alpha_{(k)}^{(r)}$ of the step 1.3;
- compute non-relaxed bounds
 - (i) with $\tilde{\mathbb{S}}$ given by the Hashin–Shtrikman bound and the initial guess given by the optimal $\mathbb{S}^{(r)}$ of the step 2.1 and
 - (ii) with $\tilde{\mathbb{S}}$ given by the self-consistent bound and the initial guess given by the optimal $\mathbb{S}^{(r)}$ of the step 2.2;

In each case, the optimization process was stopped when either the convergence criterion was met or the number of function evaluations reached 4×10^6 .

References

- Avis, D. & Fukuda, K. 1992 A pivoting algorithm for convex hulls and vertex enumeration of arrangements and polyhedra. *Discrete Comput. Geometry* **8**, 295–313. (doi:10.1007/BF02293050)
- Bishop, J. F. W. & Hill, R. 1951 A theory of the plastic distortion of a polycrystalline aggregate under combined stresses. *Phil. Mag.* **42**, 414–427.
- Bornert, M., Masson, R., Ponte Castañeda, P. & Zaoui, A. 2001 Second-order estimates for the effective behavior of viscoplastic polycrystalline materials. *J. Mech. Phys. Solids* **49**, 2737–2764. (doi:10.1016/S0022-5096(01)00077-1)
- DeBotton, G. & Ponte Castañeda, P. 1995 Variational estimates for the creep behaviour of polycrystals. *Proc. R. Soc. Lond. A* **448**, 121–142. (doi:10.1098/rspa.1995.0009)
- Bouchitté, G. & Suquet, P. 1991 Homogenization, plasticity and yield design. In *Composite media and homogenization theory* (eds G. Dal Maso & G. Dell'Antonio), pp. 107–133. Basel, Switzerland: Birkhäuser.
- Brent, R. P. 2002 *Algorithms for minimization without derivatives*. Englewood Cliffs, NJ: Prentice Hall.

- Dendievel, R., Bonnet, G. & Willis, J. R. 1991 Bounds for the creep behaviour of polycrystalline materials. In *Inelastic deformation of composite materials* (ed. G. J. Dvorak), pp. 175–192. New York, NY: Springer.
- Groves, G. W. & Kelly, A. 1963 Independent slip systems in crystals. *Phil. Mag.* **8**, 877–887. (doi:10.1080/14786436308213843)
- Hill, R. 1965 Continuum micro-mechanics of elastoplastic polycrystals. *J. Mech. Phys. Solids* **13**, 89–101. (doi:10.1016/0022-5096(65)90023-2)
- Hutchinson, J. W. 1976 Bounds and self-consistent estimates for creep of polycrystalline materials. *Proc. R. Soc. Lond. A* **348**, 101–127. (doi:10.1098/rspa.1976.0027)
- Idiart, M. I. & Ponte Castañeda, P. 2007a Variational linear comparison bounds for nonlinear composites with anisotropic phases. I. General results. *Proc. R. Soc. A* **463**, 907–924. (doi:10.1098/rspa.2006.1797)
- Idiart, M. I. & Ponte Castañeda, P. 2007b Variational linear comparison bounds for nonlinear composites with anisotropic phases. II. Crystalline materials. *Proc. R. Soc. A* **463**, 925–943. (doi:10.1098/rspa.2006.1804)
- Kocks, U. F., Canova, G. R. & Jonas, J. J. 1983 Yield vectors in F.C.C. crystals. *Acta Metall.* **31**, 1243–1252. (doi:10.1016/0001-6160(83)90186-4)
- Kocks, U. F., Tomé, C. N. & Wenk, H.-R. 1998 *Texture and anisotropy*. Cambridge, UK: Cambridge University Press.
- Lebensohn, R. A. & Tomé, C. N. 1993 A self-consistent anisotropic approach for the simulation of plastic deformation and texture development of polycrystals: application to zirconium alloys. *Acta Metall. Mater.* **41**, 2611–2624. (doi:10.1016/0956-7151(93)90130-K)
- Lebensohn, R. A., Liu, Y. & Ponte Castañeda, P. 2004 On the accuracy of the self-consistent approximation for polycrystals: comparison with full-field numerical simulations. *Acta Mater.* **52**, 5347–5361. (doi:10.1016/j.actamat.2004.07.040)
- Lebensohn, R. A., Idiart, M. I., Ponte Castañeda, P. & Vincent, P.-G. 2011 Dilatational viscoplasticity of polycrystalline solids with intergranular cavities. *Phil. Mag.* **91**, 3038–3067. (doi:10.1080/14786435.2011.561811)
- Liu, Y. & Ponte Castañeda, P. 2004 Homogenization estimates for the average behavior and field fluctuations in cubic and hexagonal viscoplastic polycrystals. *J. Mech. Phys. Solids* **52**, 1175–1211. (doi:10.1016/j.jmps.2003.08.006)
- Molinari, A., Canova, G. R. & Ahzi, S. 1987 A self-consistent approach of the large deformation polycrystal viscoplasticity. *Acta Metall. Mater.* **35**, 2983–2994. (doi:10.1016/0001-6160(87)90297-5)
- Nebozhyn, M. V., Gilormini, P. & Ponte Castañeda, P. 2000 Variational self-consistent estimates for viscoplastic polycrystals with highly anisotropic grains. *C.R. Acad. Sci. Paris Ser. II* **328**, 11–17. (doi:10.1016/S1287-4620(00)88410-0)
- Nebozhyn, M. V., Gilormini, P. & Ponte Castañeda, P. 2001 Variational self-consistent estimates for cubic viscoplastic polycrystals: the effects of grain anisotropy and shape. *J. Mech. Phys. Solids* **49**, 313–340. (doi:10.1016/S0022-5096(00)00037-5)
- Olson, T. 1994 Improvements on Taylor upper bound for rigid-plastic composites. *Mater. Sci. Eng. A* **175**, 15–20.
- Orlans-Joliet, B., Bacroix, B., Montheillet, F., Driver, J. H. & Jonas, J. J. 1988 Yield surfaces of B.C.C. crystals for slip on the {110} < 111 > and {112} < 111 > systems. *Acta Metall.* **36**, 1365–1380.
- Ponte Castañeda, P. 1991 The effective mechanical properties of nonlinear isotropic composites. *J. Mech. Phys. Solids* **39**, 45–71. (doi:10.1016/0022-5096(91)90030-R)
- Ponte Castañeda, P. & Suquet, P. 1998 Nonlinear composites. *Adv. Appl. Mech.* **34**, 171–302. (doi:10.1016/S0065-2156(08)70321-1)
- Reuss. 1929 Calculation of the flow limits of mixed crystals on the basis of the plasticity of the monocrystals. *Z. Angew. Math. Mech.* **9**, 49–58.
- Rockafellar, T. 1970 *Convex analysis*. Princeton, NJ: Princeton University Press.
- Sobol, I. M. 1967 On the distribution of points in a cube and the approximate evaluation of integrals. *USSR Comput. Math. Phys.* **7**, 86–112. (doi:10.1016/0041-5553(67)90144-9)

- Suquet, P. 1983 Analyse limite et homogénéisation. *C.R. Acad. Sci. Paris Ser. II* **296**, 1355–1358.
- Talbot, D. R. S. & Willis, J. R. 1985 Variational principles for inhomogeneous nonlinear media. *IMA J. Appl. Math.* **35**, 39–54. (doi:10.1093/imamat/35.1.39)
- Talbot, D. R. S. & Willis, J. R. 1998 Upper and lower bounds for the overall response of an elastoplastic composite. *Mech. Mater.* **28**, 1–8. (doi:10.1016/S0167-6636(97)00012-4)
- Taylor, G. I. 1938 Plastic strain in metals. *J. Inst. Metals* **62**, 307–324.
- Terzer, M. 2009 Large scale methods to enumerate extreme rays and elementary modes. Ph.D. thesis, Swiss Federal Institute of Technology, Switzerland.
- Tomé, C. & Kocks, U. F. 1985 The yield surface of H.C.P. crystals. *Acta Metall.* **33**, 603–621. (doi:10.1016/0001-6160(85)90025-2)
- Willis, J. R. 1977 Bounds and self-consistent estimates for the overall moduli of anisotropic composites. *J. Mech. Phys. Solids* **25**, 185–202. (doi:10.1016/0022-5096(77)90022-9)
- Willis, J. R. 1982 Elasticity theory of composites. In *Mechanics of solids*, The Rodney Hill 60th Anniversary volume (eds H. G. Hopkins & M. J. Sewell), pp. 653–686. Oxford, UK: Pergamon Press.
- Willis, J. R. 1983 The overall elastic response of composite materials. *J. Appl. Mech.* **50**, 1202–1209. (doi:10.1115/1.3167202)
- Willis, J. R. 1994 Upper and lower bounds for nonlinear composite behavior. *Mater. Sci. Eng. A* **175**, 7–14. (doi:10.1016/0921-5093(94)91038-3)